Available online at www.sciencedirect.com

ScienceDirect

Procedia Structural Integrity 58 (2024) 35–41

Structural Integrity Procedia

www.elsevier.com/locate/procedia

7th International Conference on Structural Integrity and Durability (ICSID 2023)

How many critical planes? A perspective insight into structural integrity

A. Chiocca[a,*], M. Sgamma[a], F. Frendo[a]

[a] *Department of Civil and Industrial Engineering, University of Pisa, Largo Lucio Lazzarino 2, Pisa 56123, Italy*

Abstract

The topic of material fatigue is a subject extensively investigated within both scientific and industrial worlds. Fatigue-induced damage remains a critical concern for a variety of components, encompassing both metallic and non-metallic materials, often leading to unexpected failures during their operational lifecycle. In cases necessitating the assessment of multiaxial fatigue, critical plane methodologies have emerged as a valuable approach. These methodologies offer the means to pinpoint the component's critical regions and anticipate early-stage crack propagation. Nevertheless, the conventional technique (i.e., plane scanning method) for computing critical plane factors is a time-intensive process, reliant on nested iterations, predominantly suited for research purposes. In numerous cases, where the critical area within a component is unknown in advance (i.e., primarily due to complex geometries and loading conditions) the method proves impractical. Furthermore, the plane scanning method does not provide a deep comprehension of the critical plane concept; indeed, it is just a numerical artifice for calculating stress and strain quantities on different planes. Recently, the authors introduced an efficient algorithm for evaluating critical plane factors. This algorithm is based on a closed form solution and is applicable to all instances where the maximization of a specific parameter, based on stress or strain components, is required. The methodology relies on tensor invariants and coordinates transformation principles thus enhancing the investigation of various critical plane methods. The paper addresses two formulations of the *Fatemi-Socie* critical plane factor and discusses how the number of critical planes depend on the loading conditions the component is subjected to. By the use of a closed form solution a deep insight of critical planes orientation can be achieved.

Keywords: critical plane; multiaxial fatigue; fatigue assessment; computational cost; algorithm efficiency; finite element analysis

1. Introduction

The topic of material fatigue is of significant importance within both the scientific and industrial communities, as evidenced by numerous studies Cowles (1989); Kaldellis and Zafirakis (2012); Koyama et al. (2017); Xu et al. (2021). A substantial number of in service failures can be attributed to fatigue mechanisms Bhaumik et al. (2008). The in-

* Corresponding author. Tel.: +39-050-2218011.
E-mail address: andrea.chiocca@unipi.it

10.1016/j.prostr.2024.05.007

herent complexities of real-world applications, such as variable amplitude loading, randomness, and multiaxial stress states, pose challenges in addressing fatigue-related issues Kuncham et al. (2022); Sgamma et al. (2023); Chiocca et al. (2020). Finite Element Analysis (FEA) has emerged as a standard practice for accommodating the complexities associated with component geometries and to accurately modeling the loading histories Frendo et al. (2020); Fontana et al. (2023); Chiocca et al. (2019, 2021, 2022a,b); Meneghetti et al. (2022). Nonetheless, simulations, particularly in the post-processing phase, can be computationally intensive. Various methods for damage assessment can be applied, including energy-based Lazzarin and Berto (2005); Berto and Lazzarin (2009); Mroziński (2019); Varvani-Farahani et al. (2007) and stress/strain-based approaches Taylor et al. (2002); Radaj et al. (2006); Findley (1959a); Socie (1987). A specific category of methodologies is founded upon the concept of the critical plane (CP) Gates and Fatemi (2017); Findley (1959b); Hemmesi et al. (2017). This local approach requires the evaluation of a designated damage factor across all conceivable orientations at each location within the model, thereby determining the point and orientation of a plane that yields the highest damage parameter value. This identified plane is named the critical plane, signifying the material orientation where crack initiation and initial propagation occur. However, implementing the CP method can be time-consuming, particularly for three-dimensional models featuring complex loading histories and geometries. This is primarily due to the necessity of scanning numerous planes within the three-dimensional space, a process that can be performed by means of nested *for/end* loops. Moreover, it may be infeasible to predefine the critical region in certain instances, especially when dealing with models characterized by highly complex geometry, load histories, and constraints. In this context, the use of optimization algorithms holds promise as a means to conduct comprehensive analyses of components.

In the current investigation, two efficient algorithms are used to evaluate different formulations of the *Fatemi-Socie* critical plane factor. By comparing the CP results with the standard plane scanning technique it is shown how the efficient algorithms could predict the number of critical planes in advance solely based on the analysis of the *eigenvalues* of the strain range tensor and without relying on the process of plane scanning.

2. Background on *Fatemi-Socie* critical plane factor

Fatemi and Socie (1988) introduced a multiaxial fatigue criterion based upon the shear strain range. The damage parameter representing the basis of the criterion is given in the following relationship (Equation 1):

$$\frac{\Delta\gamma}{2}\left(1 + k\frac{\sigma_{n,\max}}{S_y}\right) \tag{1}$$

where, $\Delta\gamma$ identifies the shear strain range acting upon a specified plane, $\sigma_{n,\max}$ denotes the maximum normal stress (over the load cycle or time interval) experienced by the plane under consideration, and S_y stands for the material's yield strength. The material parameter k is derived by comparing fatigue experimental data for uniaxial loading with data for pure torsion. It is important to emphasize that the fatigue parameter defined in Equation 1 is always positive. In fact, the absolute value of the shear strain range and only positive normal stresses are considered (i.e. negative stresses being set to zero). The original approach proposed by Fatemi and Socie (1988) identified the critical plane as the one characterized by the maximum shear strain range, $\Delta\gamma_{\max}$, as shown by the fatigue parameter FS in Equation 2. An efficient algorithm for such criteria have been addressed in prior works authored by the researchers (Chiocca et al. (2023a,c)). In addition to the FS parameter, another formulation of the *Fatemi-Socie* critical plane factor is adopted by considering the maximization of the whole fatigue parameter FS' expressed in Equation 2. It is worth noting that the critical plane, as defined in this manner, often exhibits a different orientation when compared to the critical plane defined solely based on the maximum shear strain range. The variation in CP orientation is attributed to its dependence to the normal stress. The maximization of FS' presents a distinct case, where a closed-form solution remains feasible, albeit under more stringent assumptions, as presented in Chiocca et al. (2023b).

$$FS = \frac{\Delta\gamma_{\max}}{2}\left(1 + k\frac{\sigma_{n,\max}}{S_y}\right), \quad FS' = \max\left[\frac{\Delta\gamma}{2}\left(1 + k\frac{\sigma_{n,\max}}{S_y}\right)\right] \tag{2}$$

3. Standard plane scanning method for critical plane factors evaluation

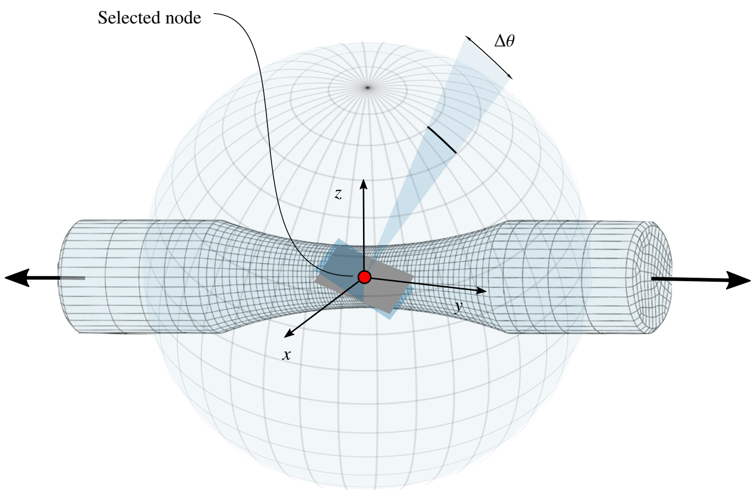

Fig. 1. Scanning plane technique applied to a generic finite element model of a loaded component.

The CP factor is determined through the analysis of stress and strain tensors. It is feasible to compute stress and strain parameters acting along distinct plane orientations, each represented by different reference coordinate systems. This computation, as exemplified in Fig. 1, can be performed through the application of matrix operations, specifically denoted as $R^T\boldsymbol{\sigma}R$, where the matrix R defines a rotation transformation and $\boldsymbol{\sigma}$ represents the stress tensor in the global reference frame. To accurately specify a plane's orientation, two angular coordinates, denoted as θ and ψ, can be used. Consequently, there exists ∞^2 plane orientations necessitating the critical plane assessment. A systematic approach involves iteratively varying the plane or its unit vector by fixed angular increments, typically denoted as $\Delta\theta$ and $\Delta\psi$, to approximate stress and strain values across all directions. Following this iterative procedure, the plane that maximizes a designated reference CP parameter can be identified as the critical plane. However, it is worth noting that the aforementioned approach entails the usage of nested *for/end* loops, which are highly inefficient from a computational perspective. This inefficiency becomes more pronounced when attempting to apply this procedure across numerous points within a component, such as nodes within a finite element models.
In the current investigation, we adopted a rotation sequence within a moving reference frame. This sequence involved a first rotation denoted as ψ about the z-axis, followed by a second rotation represented as θ about the y-axis. The plane scanning method was implemented by utilizing angular increments of $\Delta\theta$ and $\Delta\psi$, each set at 3°. The rotation sequence can be represented throughout the rotation matrix denoted as R in Equation 3. By employing the rotation matrix R stress and strain tensors can be obtained in the rotated reference frame (i.e. $\boldsymbol{\sigma'}$ and $\boldsymbol{\varepsilon'}$).

$$R = R_z(\psi)R_y(\theta) = \begin{bmatrix} \cos(\theta)\cos(\psi) & -\sin(\psi) & \cos(\psi)\sin(\theta) \\ \sin(\psi)\cos(\theta) & \cos(\psi) & \sin(\theta)\sin(\psi) \\ -\sin(\theta) & 0 & \cos(\theta) \end{bmatrix} \longrightarrow \boldsymbol{\sigma'} = R^T\boldsymbol{\sigma}R, \quad \boldsymbol{\varepsilon'} = R^T\boldsymbol{\varepsilon}R \tag{3}$$

4. Closed form solution for the critical plane factors

In order to present the efficient method, the definition of the strain range tensor (i.e. $\boldsymbol{\Delta\varepsilon}$) has to be introduced first. The strain range tensor is defined as the difference between the strain tensors at the i-th and $(i+1)$-th load steps (i.e.

$\boldsymbol{\varepsilon}^i$ and $\boldsymbol{\varepsilon}^{i+1}$) with respect to the same reference frame, as detailed in Equation 4.

$$\underbrace{\begin{bmatrix} \Delta\varepsilon_{xx} & \frac{\Delta\gamma_{xy}}{2} & \frac{\Delta\gamma_{xz}}{2} \\ \frac{\Delta\gamma_{yx}}{2} & \Delta\varepsilon_{yy} & \frac{\Delta\gamma_{yz}}{2} \\ \frac{\Delta\gamma_{zx}}{2} & \frac{\Delta\gamma_{zy}}{2} & \Delta\varepsilon_{zz} \end{bmatrix}}_{\boldsymbol{\Delta\varepsilon}} = \underbrace{\begin{bmatrix} \varepsilon_{xx} & \frac{\gamma_{xy}}{2} & \frac{\gamma_{xz}}{2} \\ \frac{\gamma_{yx}}{2} & \varepsilon_{yy} & \frac{\gamma_{yz}}{2} \\ \frac{\gamma_{zx}}{2} & \frac{\gamma_{zy}}{2} & \varepsilon_{zz} \end{bmatrix}^i}_{\boldsymbol{\varepsilon}^i} - \underbrace{\begin{bmatrix} \varepsilon_{xx} & \frac{\gamma_{xy}}{2} & \frac{\gamma_{xz}}{2} \\ \frac{\gamma_{yx}}{2} & \varepsilon_{yy} & \frac{\gamma_{yz}}{2} \\ \frac{\gamma_{zx}}{2} & \frac{\gamma_{zy}}{2} & \varepsilon_{zz} \end{bmatrix}^{i+1}}_{\boldsymbol{\varepsilon}^{i+1}} \tag{4}$$

Based on the definition of $\boldsymbol{\Delta\varepsilon}$ it is now convenient to work on the Mohr's circle representation, as presented in Fig. 2. Starting from the strain range tensor written in a generic reference frame (point 1 of Fig. 2) it is possible to obtain the principal quantities and principal directions by performing an *eigenvalues-eigenvectors* analysis ($\Delta\varepsilon_1$, $\Delta\varepsilon_2$, $\Delta\varepsilon_3$, $\mathbf{n_1}$, $\mathbf{n_2}$ and $\mathbf{n_3}$ of Fig. 2). Two different pathways open up at this point. A first case where it is required to maximize one parameter of the CP factor (e.g. FS of Equation 2) and another case where the entire CP factor needs to be maximized (e.g. FS' of Equation 2). In the first case the $\Delta\gamma_{max}$ (i.e. maximum value of FS) can be obtained, starting from the orientation representing the principal directions, by rotating of $\omega = \frac{\pi}{2}$ around the eigenvector relative to the middle eigenvalue (i.e. $\boldsymbol{n_2}$). Once the $\Delta\gamma_{max}$ is computed, the value of FS is retrieved by finding the $\sigma_{n,max}$ directly in the $\Delta\gamma_{max}$ reference system (i.e., obtained from a rotation of $\omega = \frac{\pi}{2}$ around $\boldsymbol{n_2}$).
In the second case, on the other hand, under certain simplifying assumptions of linear-elasticity and proportional loading, it occurs that the principal directions of the strain tensor range are coincident to those of the stress and strain tensors at load steps i and $i+1$. Under these assumptions the CP factor can be defined as a function of the ω angle only and therefore allowing an analytical formulation of its maximum value. The analytical formulation of FS' and of the angle $\bar{\omega}$ (i.e. identifying FS') is more complex and it requires the solution of a maximization problem. The analytical formulation of FS' employed in the following is the one presented in Chiocca et al. (2023b), under the assumptions of linear elasticity and proportional loading.

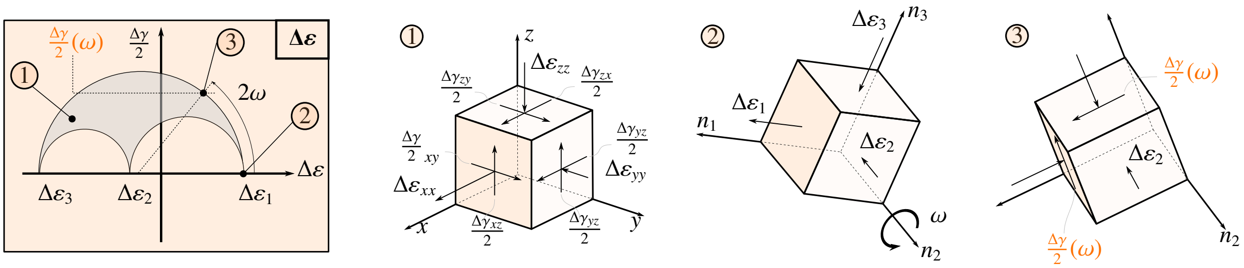

Fig. 2. Representation by means of the Mohr circles and the Cauchy elementary cube of the strain range tensor and the successive rotations required to find the plane in which $\Delta\gamma$ is maximized.

5. Test case

The case study taken as a reference is an hourglass specimen under pure tensile and fully reversed torsion loading conditions. The specimen, whose geometry is based on the ASTM E466 standard, has a minimum diameter of 12 mm. In order to apply the critical plane methods mentioned above, 2D static structural finite element simulations were developed. The material chosen was structural steel S355, characterized by linear elastic behavior with the material properties $E = 210\,\text{GPa}$ and $\nu = 0.3$. To calculate the critical plane factor denoted as FS and FS', the following material parameters were employed: a yield strength of $S_y = 355\,\text{MPa}$ and a material constant of $k = 0.4$.
In the most general case of component loading and geometry, two critical planes can always be found for both formulations of the *Fatemi-Socie* CP factor (i.e. FS and FS'). The reason relates to the use of the absolute value of $\Delta\gamma$. If observed within the Mohr circle representation of Fig. 2, retrieving the absolute value of $\Delta\gamma$ results in two permissible rotations, one of $+\omega$ and one of $-\omega$. This case occurs when all the eigenvalues of the $\boldsymbol{\Delta\varepsilon}$ tensor are different from each other. However, other special cases, where more than two critical planes exists, can be encountered.

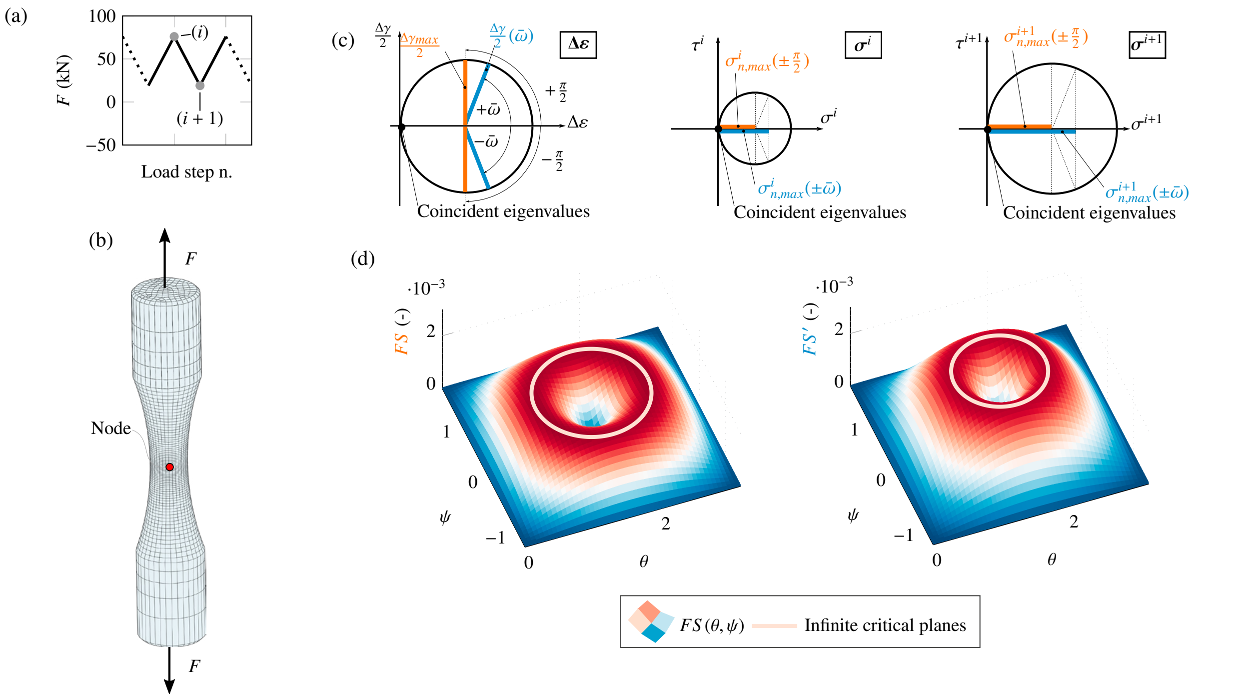

Fig. 3. Loading history (a), specimen (b), Mohr's circle representation of different tensors (c) and comparison between the plane scanning method and the efficient methods (d) for a tensile loaded component.

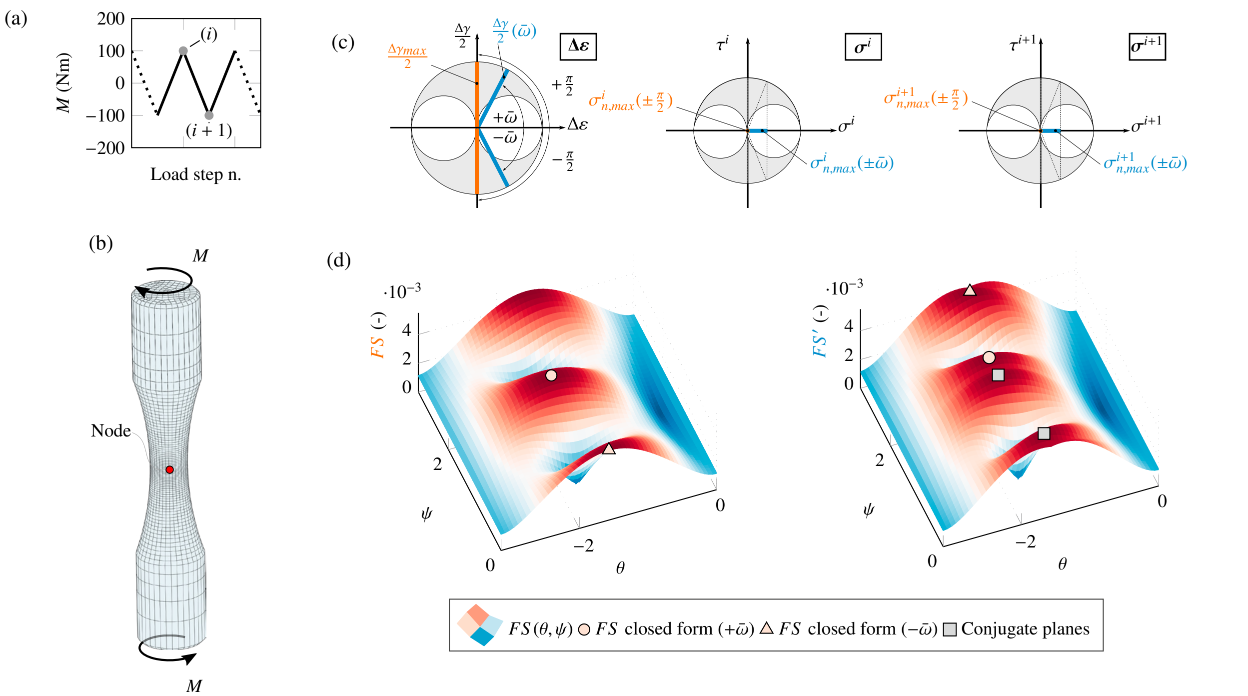

Fig. 4. Loading history (a), specimen (b), Mohr's circle representation of different tensors (c) and comparison between the plane scanning method and the efficient methods (d) for a fully reversed torsion loaded component.

A first instance is shown in Fig. 3, where an axisymmetric specimen loaded in tension is presented (Fig. 3a–b). This loading case history generates a uniaxial stress-strain state, where two eigenvalues of the $\Delta\varepsilon$ tensor are equal to zero. For this case there exist infinite critical planes for both FS and FS' formulations. In fact, the CP factors can be found by rotating of $\pm\frac{\pi}{2}$ for FS or $\pm\bar{\omega}$ for FS' about any direction that is a linear combination of the *eigenvectors* related to the null *eigenvalues*. Fig. 3c highlights the main parameters related to both *Fatemi-Socie* formulations, using the colors orange and blue, respectively for FS and FS'. Similarly, Fig. 3d presents the comparison between the efficient methods and the standard scanning plane technique for both CP formulations. The white line represents the infinite critical planes found by using the efficient method while the coloured surfaces show the iterative process of the standard plane scanning method. It can be observed that both the surfaces (i.e. plane scanning method) and the critical planes (maxima identified by the closed form solution) are slightly different for the two versions of the considered fatigue parameter. In particular the circle, representing the critical plane orientations for FS', has a slightly smaller radius if compared to FS, identifying smaller values of parameters θ and ψ.
Another load case scenario is given in Fig. 4 for a fully reversed torsion loading history (Fig. 4a) applied on a hourglass specimen (Fig. 4b). In this case, the strain range tensor and the stress tensors present two opposite *eigenvalues* as shown in Fig. 4c through the Mohr's circles. In this scenario just two critical planes are found under the FS model, while four critical planes exist under the FS' model, as shown in Fig. 4d. In fact, for each orientation there are two conjugate (orthogonal) plane which experiences the same positive normal stress, one at i-th load step and the other at $i+1$-th load step. All four planes can be obtained by rotating of $\omega = \pm\bar{\omega}$ and $\omega = \pm(\frac{\pi}{2} - \bar{\omega})$.
It is worth noting that FS' always reaches higher values respect FS as consequence of maximizing the entire factor reported in Equation 1.

6. Conclusions

This work presents a comparison between the standard plane scanning method and two efficient methods for computing the *Fatemi-Socie* critical plane factor. The efficient methods, developed by the authors as closed form solution of a maximization problem, enabled a more comprehensive analysis of the concept of critical plane factor. Indeed, they allowed the identification of the number of critical planes in advance just by comparing the *eigenvalues* of the strain range tensor. Therefore, it is not required to carry out the spatial plane scanning in order to know both the critical plane factor and the critical plane orientation. Instead it is sufficient to perform an *eigenvalues/eigenvectors* analysis of strain range and stress tensors. The analysis provides a more in-depth understanding of the critical plane factor concept by using tensor math and coordinates transformation laws with respect to the blind search-for method requiring nested *for/end* loops.

Acknowledgement

Financed by the European Union - NextGenerationEU (National Sustainable Mobility Center CN00000023, Italian Ministry of University and Research Decree n. 1033 - 17/06/2022, Spoke 11 - Innovative Materials & Lightweighting). The opinions expressed are those of the authors only and should not be considered as representative of the European Union or the European Commission's official position. Neither the European Union nor the European Commission can be held responsible for them.

References

Berto, F., Lazzarin, P., 2009. The volume-based strain energy density approach applied to static and fatigue strength assessments of notched and welded structures, in: Procedia Engineering, No longer published by Elsevier. pp. 155–158. doi:10.1016/j.proeng.2009.06.036.

Bhaumik, S.K., Sujata, M., Venkataswamy, M.A., 2008. Fatigue failure of aircraft components. Engineering Failure Analysis 15, 675–694. doi:10.1016/j.engfailanal.2007.10.001.

Chiocca, A., Frendo, F., Aiello, F., Bertini, L., 2022a. Influence of residual stresses on the fatigue life of welded joints. Numerical simulation and experimental tests. International Journal of Fatigue 162, 106901. doi:10.1016/j.ijfatigue.2022.106901.

Chiocca, A., Frendo, F., Bertini, L., 2019. Evaluation of residual stresses in a tube-to-plate welded joint. MATEC Web of Conferences 300, 19005. doi:10.1051/matecconf/201930019005.

Chiocca, A., Frendo, F., Bertini, L., 2020. Experimental evaluation of relaxed strains in a pipe-to-plate welded joint by means of incremental cutting process. Procedia Structural Integrity 28, 2157–2167. doi:10.1016/j.prostr.2020.11.043.

Chiocca, A., Frendo, F., Bertini, L., 2021. Evaluation of residual stresses in a pipe-to-plate welded joint by means of uncoupled thermal-structural simulation and experimental tests. International Journal of Mechanical Sciences 199, 106401. doi:10.1016/j.ijmecsci.2021.106401.

Chiocca, A., Frendo, F., Marulo, G., 2023a. An efficient algorithm for critical plane factors evaluation. International Journal of Mechanical Sciences 242, 107974. doi:10.1016/j.ijmecsci.2022.107974.

Chiocca, A., Sgamma, M., Frendo, F., 2023b. Closed-form solution for the Fatemi-Socie extended critical plane parameter in case of linear elasticity and proportional loading. Fatigue & Fracture of Engineering Materials & Structures doi:10.1111/FFE.14153.

Chiocca, A., Sgamma, M., Frendo, F., Bucchi, F., 2023c. Rapid and accurate fatigue assessment by an efficient critical plane algorithm: application to a FSAE car rear upright. Procedia Structural Integrity 47, 749–756. doi:10.1016/J.PROSTR.2023.07.044.

Chiocca, A., Tamburrino, F., Frendo, F., Paoli, A., 2022b. Effects of coating on the fatigue endurance of FDM lattice structures. Procedia Structural Integrity 42, 799–805. doi:10.1016/j.prostr.2022.12.101.

Cowles, B.A., 1989. High cycle fatigue in aircraft gas turbines—an industry perspective. International Journal of Fracture 80, 147–163. doi:10.1007/BF00012667.

Fatemi, A., Socie, D.F., 1988. A critical plane approach to multiaxial fatigue damage including out-of-phase loading. Fatigue and Fracture of Engineering Materials and Structures 11, 149–165. doi:10.1111/j.1460-2695.1988.tb01169.x.

Findley, W.N., 1959a. A Theory for the Effect of Mean Stress on Fatigue of Metals Under Combined Torsion and Axial Load or Bending. Journal of Engineering for Industry 81, 301–305. doi:10.1115/1.4008327.

Findley, W.N., 1959b. A Theory for the Effect of Mean Stress on Fatigue of Metals Under Combined Torsion and Axial Load or Bending. Journal of Engineering for Industry 81, 301–305. doi:10.1115/1.4008327.

Fontana, F., Chiocca, A., Sgamma, M., Bucchi, F., Frendo, F., 2023. Numerical-experimental characterization of the dynamic behavior of PCB for the fatigue analysis of PCBa. Procedia Structural Integrity 47, 757–764. doi:10.1016/J.PROSTR.2023.07.043.

Frendo, F., Marulo, G., Chiocca, A., Bertini, L., 2020. Fatigue life assessment of welded joints under sequences of bending and torsion loading blocks of different lengths. Fatigue and Fracture of Engineering Materials and Structures 43, 1290–1304. doi:10.1111/ffe.13223.

Gates, N.R., Fatemi, A., 2017. On the consideration of normal and shear stress interaction in multiaxial fatigue damage analysis. International Journal of Fatigue 100, 322–336. doi:10.1016/j.ijfatigue.2017.03.042.

Hemmesi, K., Farajian, M., Fatemi, A., 2017. Application of the critical plane approach to the torsional fatigue assessment of welds considering the effect of residual stresses. International Journal of Fatigue 101, 271–281. doi:10.1016/j.ijfatigue.2017.01.023.

Kaldellis, J.K., Zafirakis, D.P., 2012. Trends, prospects, and r&d directions in wind turbine technology, in: Comprehensive Renewable Energy. Elsevier. volume 2, pp. 671–724. doi:10.1016/B978-0-08-087872-0.00224-9.

Koyama, M., Zhang, Z., Wang, M., Ponge, D., Raabe, D., Tsuzaki, K., Noguchi, H., Tasan, C.C., 2017. Bone-like crack resistance in hierarchical metastable nanolaminate steels. Science 355, 1055–1057. doi:10.1126/science.aal2766.

Kuncham, E., Sen, S., Kumar, P., Pathak, H., 2022. An online model-based fatigue life prediction approach using extended Kalman filter. Theoretical and Applied Fracture Mechanics 117, 103143. doi:10.1016/j.tafmec.2021.103143.

Lazzarin, P., Berto, F., 2005. Some expressions for the strain energy in a finite volume surrounding the root of blunt V-notches. International Journal of Fracture 135, 161–185. doi:10.1007/s10704-005-3943-6.

Meneghetti, G., Campagnolo, A., Visentin, A., Avalle, M., Benedetti, M., Bighelli, A., Castagnetti, D., Chiocca, A., Collini, L., De Agostinis, M., De Luca, A., Dragoni, E., Fini, S., Fontanari, V., Frendo, F., Greco, A., Marannano, G., Moroni, F., Pantano, A., Pirondi, A., Rebora, A., Scattina, A., Sepe, R., Spaggiari, A., Zuccarello, B., 2022. Rapid evaluation of notch stress intensity factors using the peak stress method with 3D tetrahedral finite element models: Comparison of commercial codes. Fatigue and Fracture of Engineering Materials and Structures 45, 1005–1034. doi:10.1111/ffe.13645.

Mroziński, S., 2019. Energy-based method of fatigue damage cumulation. International Journal of Fatigue 121, 73–83. doi:10.1016/j.ijfatigue.2018.12.008.

Radaj, D., Sonsino, C.M., Fricke, W., 2006. Fatigue Assessment of Welded Joints by Local Approaches: Second Edition. doi:10.1533/9781845691882.

Sgamma, M., Chiocca, A., Bucchi, F., Frendo, F., 2023. Frequency analysis of random fatigue: Setup for an experimental study. Applied Research , e202200066doi:10.1002/appl.202200066.

Socie, D., 1987. Multiaxial fatigue damage models. Journal of Engineering Materials and Technology, Transactions of the ASME 109, 293–298. doi:10.1115/1.3225980.

Taylor, D., Barrett, N., Lucano, G., 2002. Some new methods for predicting fatigue in welded joints. International Journal of Fatigue 24, 509–518. doi:10.1016/S0142-1123(01)00174-8.

Varvani-Farahani, A., Haftchenari, H., Panbechi, M., 2007. An energy-based fatigue damage parameter for off-axis unidirectional FRP composites. Composite Structures 79, 381–389. doi:10.1016/j.compstruct.2006.02.013.

Xu, L., Wang, K., Yang, X., Su, Y., Yang, J., Liao, Y., Zhou, P., Su, Z., 2021. Model-driven fatigue crack characterization and growth prediction: A two-step, 3-D fatigue damage modeling framework for structural health monitoring. International Journal of Mechanical Sciences 195, 106226. doi:10.1016/j.ijmecsci.2020.106226.